

See discussions, stats, and author profiles for this publication at: <https://www.researchgate.net/publication/251606926>

# Spectral studies on Cr <sup>3+</sup> ions doped in sodium–lead borophosphate glasses

ARTICLE *in* PHYSICA B CONDENSED MATTER · MAY 2011

Impact Factor: 1.32 · DOI: 10.1016/j.physb.2011.02.051

---

CITATIONS

8

---

READS

45

4 AUTHORS, INCLUDING:



C. R. Kesavulu

Kyungpook National University

21 PUBLICATIONS 262 CITATIONS

SEE PROFILE



# Spectral studies on $\text{Cr}^{3+}$ ions doped in sodium–lead borophosphate glasses

N. Kiran<sup>a</sup>, C.R. Kesavulu<sup>b</sup>, A. Suresh Kumar<sup>a</sup>, J.L. Rao<sup>b,\*</sup>

<sup>a</sup> University Science Instrumentation Center, S.V. University, Tirupati 517 502, India

<sup>b</sup> Department of Physics, S.V. University, Tirupati 517 502, India

## ARTICLE INFO

### Article history:

Received 8 November 2010

Received in revised form

17 February 2011

Accepted 18 February 2011

Available online 24 February 2011

### Keywords:

$\text{Cr}^{3+}$  ions

Sodium–lead borophosphate glasses

Electron paramagnetic resonance

## ABSTRACT

Electron paramagnetic resonance (EPR), optical absorption and emission spectra of  $\text{Cr}^{3+}$  ions doped in  $(30-x)(\text{NaPO}_3)_6 + 30\text{PbO} + 40\text{B}_2\text{O}_3 + x\text{Cr}_2\text{O}_3$  ( $x=0.5, 2.0, 3.0, 4.0$  and  $5.0$  mol%) glasses have been studied. The EPR spectra exhibit resonance signals with effective  $g$  values at  $g \approx 4.55$  and  $g \approx 1.97$ . The EPR spectra of  $x=3.0$  mol% of  $\text{Cr}_2\text{O}_3$  in sodium–lead borophosphate glass sample were studied at various temperatures (295–123 K). The intensity of the resonance signals increases with decrease in temperature. The optical absorption spectrum exhibits four bands characteristic of  $\text{Cr}^{3+}$  ions in octahedral symmetry. From the analysis of the bands, the crystal-field parameter  $Dq$  and the Racah interelectronic repulsion parameters  $B$  and  $C$  have been evaluated. The emission spectrum exhibit one broad band characteristic of  $\text{Cr}^{3+}$  ions in octahedral symmetry. This band has been assigned to the transition  ${}^4\text{T}_{2g}(\text{F}) \rightarrow {}^4\text{A}_{2g}(\text{F})$ . Correlating EPR and optical data, the molecular bonding coefficient ( $\alpha$ ) has been evaluated.

© 2011 Elsevier B.V. All rights reserved.

## 1. Introduction

Chromium ions with  $3d^3$  configuration are of interest for solid state laser materials due to their ability to generate laser emission in the near infrared spectral region between 1.2 and  $1.7 \mu\text{m}$  [1]. In recent years, renewed studies on optical performances of  $\text{Cr}^{3+}$  ions in crystals and glasses have been reported because of the exploitation of these materials as active media for infrared tunable lasers, and to aid the fundamental understanding of the interaction between impurity and host lattice [2,3]. Among glasses, phosphate glasses have been of large interest for a variety of technological applications due to several unique properties such as high thermal expansion coefficient, low viscosity, low chemical durability, UV transmission or electrical conduction [4–6]. The addition of boron oxide improves the high chemical durability of borophosphate glasses [7]. Koudelka et al. [8] reported the study of structural changes in the  $\text{Na}_2\text{O}-\text{PbO}-\text{B}_2\text{O}_3-\text{P}_2\text{O}_5$  system glasses using NMR, Raman and IR spectroscopy techniques.

In the present study, the authors report the investigation of chromium ions in the sodium–lead borophosphate glass matrices using electron paramagnetic resonance (EPR), optical absorption and emission techniques. The authors are also interested to know the variation of EPR line intensity with temperature, which allows one to calculate the exchange-interaction energy ( $J$ ) between chromium ions. The results obtained from these studies are discussed in detail.

## 2. Experimental

The glass samples studied in the present work were obtained by the melt quenching technique. The glasses were prepared by mixing and grinding together appropriate amounts of  $(\text{NaPO}_3)_6$ ,  $\text{PbO}$ ,  $\text{B}_2\text{O}_3$  and  $\text{Cr}_2\text{O}_3$  in an agate mortar before transferring to a porcelain crucible. The mixtures were heated in an electrical furnace in air at 1223 K for 30 min.

The EPR spectra were recorded at room temperature using a JEOL-FE1X EPR spectrometer operating at the X-band frequency (9.205 GHz) with a field modulation frequency of 100 kHz. The EPR spectrum of glass sample was recorded at different temperatures (123–295 K) using a variable temperature controller (JES UCT 2AX).

The optical absorption measurements were carried out in the 200–850 nm range with 0.1 nm resolution, on a JASCO (UV–vis–NIR) spectrophotometer. The luminescence spectrum was obtained in the wavelength range 600–850 nm by exciting the sample at 448 nm using JOBIN YUON Fluorolog-3 Spectrofluorimeter using Xenon flash lamp as radiation source.

## 3. Results and analysis

### 3.1. EPR studies

No EPR signal was detected in the spectra of undoped glasses, indicating that the starting materials used in the present work were free from transition metal impurities (or paramagnetic defects). When  $\text{Cr}^{3+}$  ions with different concentrations ( $x=0.5, 2.0, 3.0, 4.0$  and  $5.0$  mol%) are introduced into

\* Corresponding author. Tel.: +91 877 2249666x272; fax: +91 877 2249611/2249532.

E-mail address: [jlrao46@yahoo.co.in](mailto:jlrao46@yahoo.co.in) (J.L. Rao).

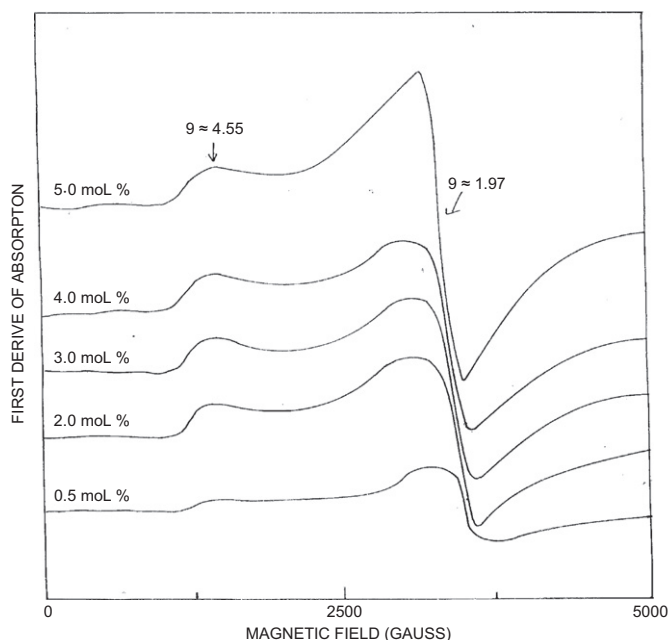


Fig. 1. EPR spectra of  $\text{Cr}_2\text{O}_3$  doped  $(30-x) (\text{NaPO}_3)_6+30\text{PbO}+40\text{B}_2\text{O}_3+x\text{Cr}_2\text{O}_3$  ( $x=0.5, 2.0, 3.0, 4.0$  and  $5.0$  mol%) glasses at room temperature.

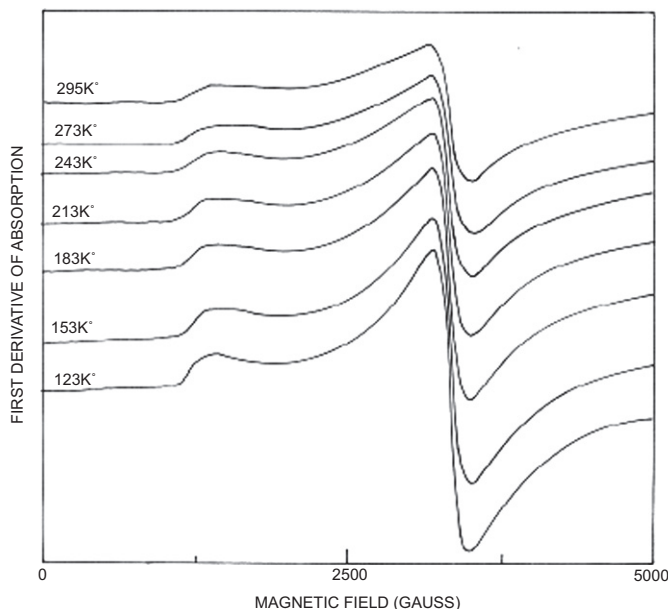


Fig. 2. EPR spectra of  $27(\text{NaPO}_3)_6+30\text{PbO}+40\text{B}_2\text{O}_3+3\text{Cr}_2\text{O}_3$  glass sample at various low temperatures.

$(30-x) (\text{NaPO}_3)_6+30\text{PbO}+40\text{B}_2\text{O}_3+x\text{Cr}_2\text{O}_3$  sodium–lead borophosphate glasses (referred as NaPbBP), the EPR spectra of all the investigated samples exhibit two resonance signals at room temperature and are shown in Fig. 1. The EPR spectrum exhibits weak and low field resonance signal with effective  $g$  value at  $g \approx 4.55$  and a strong high field resonance signal at  $g \approx 1.97$ .

The EPR spectra of NaPbBP: $3.0\text{Cr}^{3+}$  mol% glass sample were also studied at various low temperatures (123–295 K) and the spectra are shown in Fig. 2. It is observed that the resonance signal intensities decrease with increase in temperature.

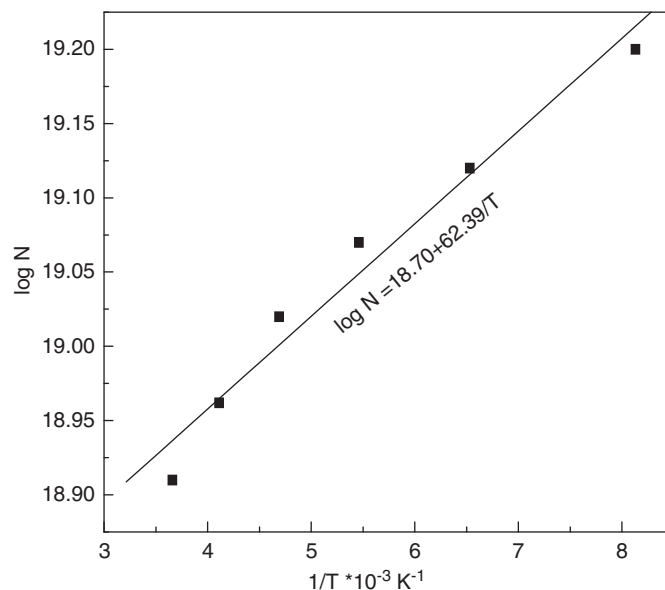


Fig. 3. A plot of reciprocal of  $\log N$  versus  $1/T$  for  $27(\text{NaPO}_3)_6+30\text{PbO}+40\text{B}_2\text{O}_3+3\text{Cr}_2\text{O}_3$  glass sample.

### 3.2. Population difference between Zeeman levels ( $N$ )

The population difference between Zeeman levels ( $N$ ) can be calculated by comparing the area under the absorption curve with that of a standard ( $\text{CuSO}_4 \cdot 5\text{H}_2\text{O}$  in this study) of known concentration. Weil et al. [9] gave the following expression, which includes the experimental parameters of both sample and standard:

$$N = \frac{A_x(\text{Scan}_x)^2 G_{\text{std}}(B_m)_{\text{std}}(g_{\text{std}})^2 [S(S+1)]_{\text{std}} (P_{\text{std}})^{1/2}}{A_{\text{std}}(\text{Scan}_{\text{std}})^2 G_x(B_m)_x (g_x)^2 [S(S+1)]_x (P_x)^{1/2}} [\text{Std}] \quad (1)$$

where  $A$  is the area under the absorption curve, which can be obtained by double integrating the first derivative EPR absorption curve,  $\text{Scan}$  is the magnetic field corresponding to a unit length of the chart,  $G$  is the gain,  $B_m$  is the modulation field width,  $g$  is the  $g$  factor,  $S$  is the spin of the system in its ground state and  $P$  is the power of the microwave source. The subscripts ' $x$ ' and ' $\text{std}$ ' represent the corresponding quantities for the NaPbBP: $\text{Cr}^{3+}$  glass sample and the reference ( $\text{CuSO}_4 \cdot 5\text{H}_2\text{O}$ ), respectively. Since the EPR signal at  $g \approx 1.97$  is intense, this  $g$  value is used to calculate the population difference between Zeeman levels ( $N$ ) at different temperatures. Fig. 3 shows a plot of  $\log N$  against  $1/T$ .

### 3.3. Calculation of paramagnetic susceptibility ( $\chi$ ) from EPR data

The magnetic susceptibility ( $\chi$ ) of  $\text{Cr}^{3+}$  ions has been calculated at different temperatures using the expression [10]:

$$\chi = \frac{Ng^2\beta^2J(J+1)}{3k_B T} \quad (2)$$

where  $N$  is the number of spins per  $\text{m}^3$ ,  $g$  is the spectroscopic splitting factor,  $\beta$  is the Bohr magneton,  $k_B$  is the Boltzmann constant and  $J=3/2$ .  $N$  can be calculated from Eq. (1) and  $g=1.97$  is taken from EPR data. The paramagnetic susceptibility was calculated at room and different temperatures. A plot of the reciprocal of susceptibility ( $1/\chi$ ) as a function of absolute temperature  $T$  is shown in Fig. 4.

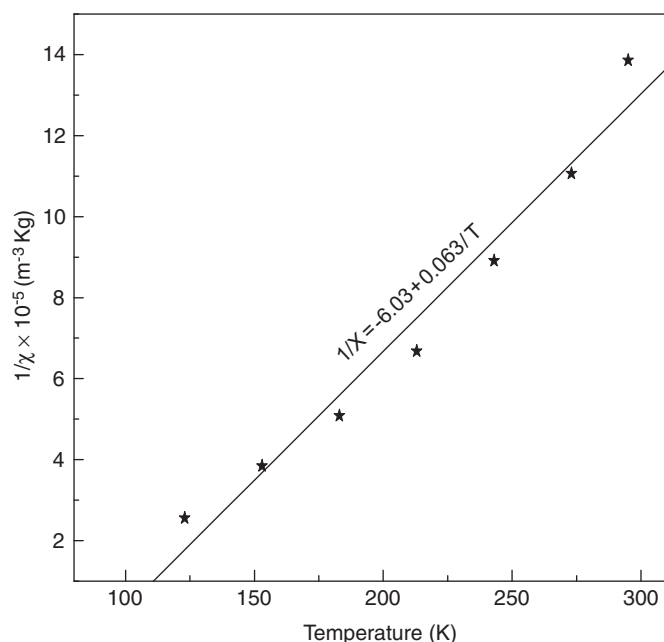


**Fig. 4.** A plot of reciprocal of susceptibility as a function of absolute temperature for  $27(\text{NaPO}_3)_6+30\text{PbO}+40\text{B}_2\text{O}_3+3\text{Cr}_2\text{O}_3$  glass sample.

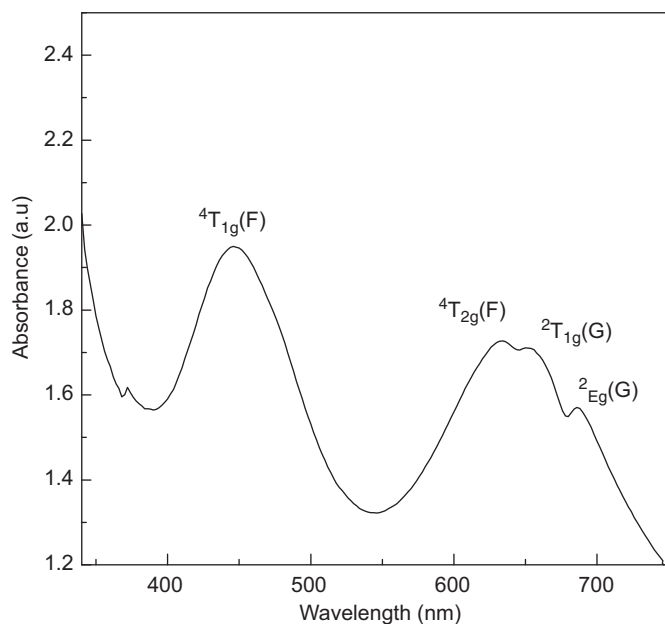


**Fig. 5.** Optical absorption spectrum of  $29.5(\text{NaPO}_3)_6+30\text{PbO}+40\text{B}_2\text{O}_3+0.5\text{Cr}_2\text{O}_3$  glass sample at room temperature.

### 3.4. Absorption and emission studies

The optical absorption spectrum of  $\text{NaPbBP:0.5 mol\% Cr}^{3+}$  ion glass sample in the wavelength region 200–800 nm is shown in Fig. 5. The spectrum exhibits four bands centered at 447 nm ( $22,370 \text{ cm}^{-1}$ ), 632 nm ( $15,822 \text{ cm}^{-1}$ ), 653 nm ( $15,315 \text{ cm}^{-1}$ ) and 687 nm ( $14,555 \text{ cm}^{-1}$ ). Among these, the band at 447 nm is the most intense one.

The luminescence spectrum of  $\text{NaPbBP:0.5 mol\% Cr}^{3+}$  glass excited at 448 nm is shown in Fig. 6. The emission spectrum exhibits a broad band centered at 720 nm ( $13,888 \text{ cm}^{-1}$ ).

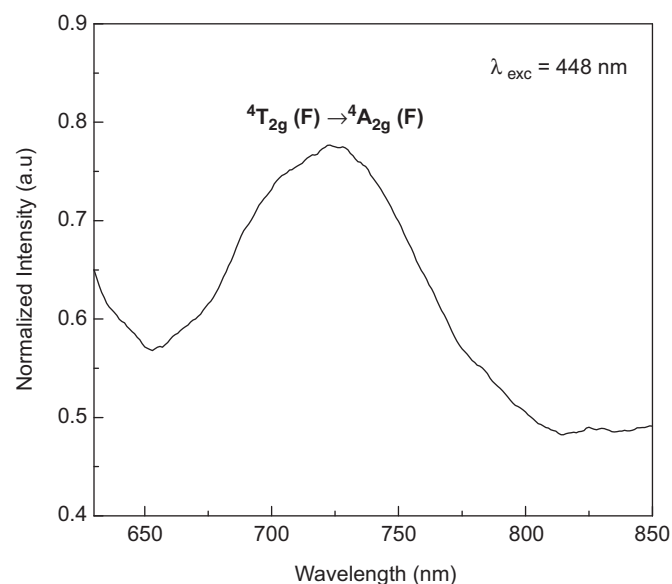


**Fig. 6.** Luminescence spectrum of  $29.5(\text{NaPO}_3)_6+30\text{PbO}+40\text{B}_2\text{O}_3+0.5\text{Cr}_2\text{O}_3$  glass sample at room temperature.

## 4. Discussion

### 4.1. EPR studies

$\text{Cr}^{3+}$  ions belong to  $3d^3$  electronic configuration. The axial distortion of octahedral symmetry gives rise to two Kramers doublets ( $M_s = \pm 3/2$  and  $M_s = \pm 1/2$ ). Application of Zeeman field lifts the spin degeneracy of these Kramers doublets. As the crystal field splitting is normally much greater than the Zeeman field, the resonance signals observed are due to transition within the Zeeman field split Kramers doublets [11].

EPR spectra of  $\text{Cr}^{3+}$  ions in borate [12], borotellurite [13] and borosulphate [14] glasses were reported by many authors. In all these glasses two resonance signals were observed at  $g \approx 5.0$  and  $g \approx 2.0$ ; these resonance signals have been attributed to isolated  $\text{Cr}^{3+}$  ions in strongly distorted sites and  $\text{Cr}^{3+}$  ion pairs, respectively. Recently Kesavulu et al. [15] studied the EPR spectra of  $\text{Cr}^{3+}$  ions in borophosphate glasses at room and low temperatures. They reported resonance signals with effective  $g$  values at  $g=4.56$  and  $g=1.96$  for borophosphate glasses. In the present work, the authors observed the resonance signals in the vicinity of  $g \approx 4.55$  and  $g \approx 1.97$  (Figs. 1 and 2). The resonance signal at  $g \approx 4.55$  is assigned to the isolated  $\text{Cr}^{3+}$  ions. The intense resonance signal at  $g \approx 1.97$  may be due to both exchange coupled  $\text{Cr}^{3+}$  ions and isolated  $\text{Cr}^{3+}$  ions.

Fig. 3 shows a plot of logarithmic dependence of the number of spins ( $\log N$ ) participating in resonance against the reciprocal of absolute temperature ( $1/T$ ). From the plot, it is seen that as the temperature is lowered, the population difference between Zeeman levels increases and a linear relationship is observed in a plot between  $\log N$  versus  $1/T$ , obeying the Boltzmann distribution law. The data is a least squares fit to straight line  $\log N = 18.70 + (62.39/T)$ . The activation energy is calculated and is found to be  $2.867 \times 10^{-21} \text{ J}$  (i.e.,  $0.012 \text{ eV}$ ), which is of the same order expected for a paramagnetic ion [15].

Fig. 4 shows a plot of the variation of the reciprocal of susceptibility against absolute temperature in  $\text{NaPbBP:Cr}^{3+}$  glass sample. The curve is fitted to a straight line. It is interesting to note that with increase in temperature, the susceptibility of the sample decreases obeying the Curie–Weiss law. From the graph, it is observed that the  $\text{NaPbBP:Cr}^{3+}$  sample follows a Curie–Weiss

type of behavior ( $\chi = C/(T - \theta_p)$ ) and the Curie constant ( $C$ ) and the paramagnetic Curie temperature ( $\theta_p$ ) have been evaluated and are found to be 95.71 emu/mol and  $\theta_p = 110$  K, respectively. The Curie constant and Curie temperature values obtained in the present work are in good agreement with the values reported in literature for paramagnetic ions [16].

#### 4.2. Exchange coupling constant ( $J$ ) between $\text{Cr}^{3+}$ pairs

Fournier et al. [17] gave the following expression to calculate the relative intensity at various temperatures:

$$I(T) = \frac{4\exp(-J/kT) + 20\exp(-3J/kT) + 56\exp(-6J/kT)}{1 + 3\exp(-J/kT) + 5\exp(-3J/kT) + 7\exp(-6J/kT)} \quad (3)$$

where ( $J$ ) is the exchange coupling constant between  $\text{Cr}^{3+}$  ion pairs,  $k$  is the Boltzmann constant and  $T$  is the absolute temperature. The intensities were determined by double integrating the EPR first derivative curve. The relative intensities were measured with respect to the intensity at room temperature. Fig. 7 shows a plot of a relative intensity  $I(T)$  versus  $kT$  for different  $J$  values calculated using Eq. (3). Fig. 7 also shows the experimental values superimposed on theoretical curves. Fournier et al. [17] have taken spin  $S=1/2$  for the samples as a standard for measuring relative intensities. In the present work the relative intensities were measured with respect to the intensity at room temperature. Hence, all the curves have been scaled to a factor of 10 at room temperature (corresponding to  $kT=209 \text{ cm}^{-1}$ ). Fig. 7 shows that the experimental data is very close to the curve for  $J=200 \text{ cm}^{-1}$ . This value is in the same order as reported by Murali and Lakshmana Rao [18].

Fournier et al. [17] observed that the intensity of the resonance signal at  $g=1.97$  increases with increase in temperature, if exchange is antiferromagnetic. In the present study, the authors observed, in contrast to Fournier et al. [17], a decrease in signal intensity with increase in temperature. The decrease in intensity with increase in temperature is possible only if the exchange interaction between  $\text{Cr}^{3+}$  ion pairs is ferromagnetic in nature. Hence, in the present case the  $g \approx 1.97$  resonance line is attributed to the  $\text{Cr}^{3+}$  pairs coupled through ferromagnetic interaction.

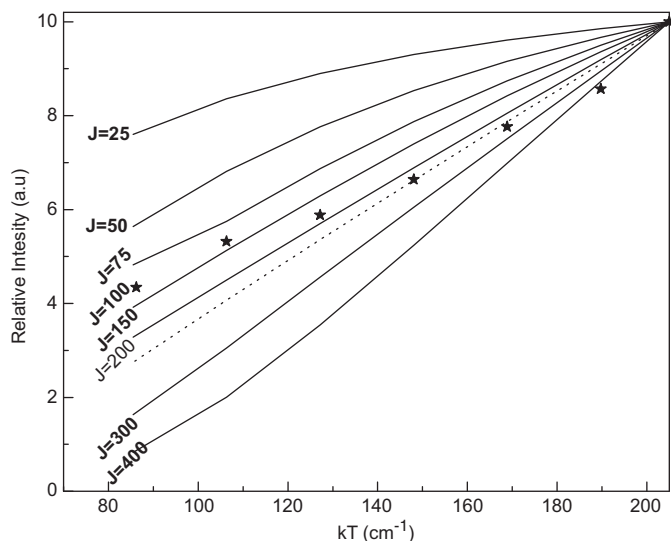


Fig. 7. Variation of relative intensity of EPR spectra with  $kT$  for different  $J$  values. The experimental points are superimposed. The stars indicate the experimental relative intensities.

#### 4.3. Optical absorption and emission studies

The ground state electronic configuration of  $\text{Cr}^{3+}$  ions gives rise to the free ion terms  $^4F$ ,  $^4P$ ,  $^2G$  and several other doublet states out of which  $^4F$  is the ground state. In octahedral coordinated system, in the weak crystal fields,  $^4F$  splits as  $^4A_{2g}(F)$ ,  $^4T_{2g}(F)$  and  $^4T_{1g}(F)$ , whereas  $^4P$  transforms as  $^4T_{1g}(P)$ . In the doublet states,  $^2G$  splits as  $^2A_{1g}(G)$ ,  $^2E_g(G)$ ,  $^2T_{1g}(G)$  and  $^2T_{2g}(G)$ . The weak field terms  $^4A_{2g}(F)$ ,  $^2E_g(G)$ ,  $^2T_{1g}(G)$  and  $^2T_{2g}(G)$  correspond to the lowest strong field configuration  $(t_{2g})^3$ . The ground state is  $^4A_{2g}(F)$  at all strengths of the crystal field. Thus only three spin allowed transitions arise from  $^4A_{2g}(F)$  to  $^4T_{2g}(F)$ ,  $^4T_{1g}(F)$  and  $^4T_{1g}(P)$  states, in addition to several spin forbidden transitions [19]. Among the above observed spectral bands, two bands located at 22,370 and 15,822  $\text{cm}^{-1}$  are assigned to spin allowed transitions  $^4A_{2g}(F) \rightarrow ^4T_{1g}(F)$  and  $^4A_{2g}(F) \rightarrow ^4T_{2g}(F)$ , respectively. The other two bands observed at 15,315 and 14,555  $\text{cm}^{-1}$  are attributed to spin forbidden transitions  $^4A_{2g}(F) \rightarrow ^2T_{1g}(G)$  and  $^4A_{2g}(F) \rightarrow ^2E_g(G)$ , respectively.

The crystal field parameter  $Dq$  is evaluated from the band position of  $^4A_{2g}(F) \rightarrow ^4T_{2g}(F)$  as

$$Dq = \frac{E(^4A_{2g}(F) - ^4T_{2g}(F))}{10}$$

The value of Racah interelectronic repulsion parameter is evaluated using the relations given by Casalbani et al. [20]:

$$\frac{Dq}{B} = \frac{15(X-8)}{(X^2-10X)}$$

where  $X = (E_1 - E_2)/Dq$ .

Here  $E_1$  and  $E_2$  represent the energies of  $^4A_{2g}(F) \rightarrow ^4T_{1g}(F)$  and  $^4A_{2g}(F) \rightarrow ^4T_{2g}(F)$  transitions, respectively. The crystal field parameter  $Dq$  evaluated is found to be 1582  $\text{cm}^{-1}$ . This value is in the expected order for  $\text{Cr}^{3+}$  ions in octahedral symmetry [21,22]. The parameter  $B$  is found to be  $B=662 \text{ cm}^{-1}$ . The value of interelectronic repulsion parameter  $B$  for the  $\text{Cr}^{3+}$  free ion is 918  $\text{cm}^{-1}$  [23]. A comparison with the observed  $B$  value (662  $\text{cm}^{-1}$ ) indicates that the  $B$  value is decreased by 28%. This might be due to bonding effects. In weak crystal field site, the value of  $(Dq/B) < 2.3$ ; in strong crystal field site  $(Dq/B) > 2.3$ . For intermediate crystal field  $(Dq/B) = 2.3$  [24,25]. In the present work, the ratio of  $Dq/B$  is found to be 2.39. Similar ratio has been reported for  $\text{Cr}^{3+}$  ions for other glass systems and this suggests that the  $\text{Cr}^{3+}$  ions are situated in intermediate crystal field [15,26,27].

The energy matrices for  $d^3$  configuration have been diagonalized for values of  $Dq$ ,  $B$  and  $C$ , and a good fit is obtained for  $Dq=1582 \text{ cm}^{-1}$ ;  $B=662 \text{ cm}^{-1}$ ; and  $C=3217 \text{ cm}^{-1}$ . The observed and calculated energies of the bands are presented in Table 1.

EPR and optical absorption data can be correlated to evaluate the molecular bonding coefficient ( $\alpha$ ) using the formula [28]:

$$g_0 = g_e - 8\alpha\lambda/\Delta$$

Here  $g_e$  is the free electron  $g$  factor ( $g_e=2.0023$ ) and  $g_0$  is the experimental  $g$  value obtained in the present work ( $g_{\text{eff}}=1.97$ ),  $\lambda$  is the spin-orbit coupling constant for free  $\text{Cr}^{3+}$  ions (90  $\text{cm}^{-1}$ ) and

Table 1

Observed and calculated band positions along with their assignments for  $\text{Cr}^{3+}$  ions in sodium-lead borophosphate glass sample ( $Dq=1582 \text{ cm}^{-1}$ ,  $B=662 \text{ cm}^{-1}$  and  $C=3217 \text{ cm}^{-1}$ ).

Transition from $^4A_{2g}(F)$ to	Observed		Calculated wavenumber ( $\text{cm}^{-1}$ )
	Wavelength (nm)	Wavenumber ( $\text{cm}^{-1}$ )	
$^4T_{1g}(F)$	447	22,370	22,362
$^4T_{2g}(F)$	632	15,822	15,822
$^2T_{1g}(G)$	653	15,315	15,000
$^2E_g(G)$	687	14,555	14,620

$\Delta$  is the energy difference between the ground and excited electronic levels. The parameter  $\alpha$  is characteristic of the ionic contribution to the chemical bond between  $\text{Cr}^{3+}$  ion and the ligands. The larger the value of  $\alpha$ , the stronger the ionic contribution to the chemical bond and the smaller the value of  $g$  factor. The obtained values of  $\alpha$  ( $\approx 0.70$ ) and the  $g$  value indicate that the bonding between the  $\text{Cr}^{3+}$  ions and the ligands is moderately ionic.

A broad emission band is obtained at 720 nm ( $13,888 \text{ cm}^{-1}$ ) when the sample is excited at a wave length of 448 nm. In most of the glass samples, only one emission band is reported at room temperature [29–32]. In the present work, the broad emission band is assigned to the transition  ${}^4\text{T}_{2g}(\text{F}) \rightarrow {}^4\text{A}_{2g}(\text{F})$ , which is expected for  $\text{Cr}^{3+}$  ions in octahedral symmetry [33].

## 5. Conclusions

EPR spectra of  $\text{Cr}^{3+}$  ions doped sodium–lead borophosphate glasses exhibit two resonance signals with effective  $g$  values at  $g \approx 4.55$  and  $g \approx 1.97$ , and these signals are attributed to isolated  $\text{Cr}^{3+}$  ions and exchange coupled  $\text{Cr}^{3+}$  pairs, respectively. The population of difference between Zeeman levels participating in resonance exhibits a linear relationship between  $\log N$  and  $1/T$  obeying the Boltzmann distribution law. The reciprocal of susceptibility with temperature obeys the Curie–Weiss law. By measuring the relative intensity of the EPR signal at  $g=1.97$  at various temperatures, the exchange coupling constant ( $J$ ) has been estimated. The optical absorption spectrum exhibits four bands characteristic of  $\text{Cr}^{3+}$  ions in nearly octahedral sites. From the position of the absorption band maxima, the crystal-field splitting and Racah parameters ( $B$  and  $C$ , respectively) have been evaluated. By correlating EPR and optical absorption data, the molecular bonding coefficient  $\alpha$  has been calculated. The calculated value of  $\alpha$  suggests that the bonding between  $\text{Cr}^{3+}$  ions and the ligands is moderately ionic. The emission spectrum exhibits a broad band expected for  $\text{Cr}^{3+}$  ions in the octahedral symmetry.

## References

- [1] G. Yang, Q. Zhang, D. Shi, Z. Jiang, J. Am. Ceram. Soc. 90 (2007) 309.
- [2] M. Casalbani, A. Luci, U.M. Grassano, B.V. Mill, A. Kaminskii, Phys. Rev. B 49 (1994) 3781.
- [3] A. Kaminskii, A. Suchocki, L. Arizmendi, D. Callejo, F. Jaque, M. Grinberg, Phys. Rev. B 62 (2000) 10802.
- [4] Y.M. Moustala, K. El-Egili, J. Non-Cryst. Solids 240 (1998) 144.
- [5] R.K. Brow, J. Non-Cryst. Solids 1 (2000) 263.
- [6] M.I. Abd El-Ati, A.A. Higazy, J. Mater. Sci. 35 (2000) 6175.
- [7] L. Koudelka, P. Mošner, M. Zeyer, C. Jäger, Phys. Chem. Glasses 43 (2002) 102.
- [8] L. Koudelka, P. Mošner, M. Zeyer, C. Jäger, J. Non-Cryst. Solids 351 (2005) 1039.
- [9] J.A. Weil, J.R. Bolton, J.E. Wertz, Electron Paramagnetic Resonance—Elementary, Theory and Practical Application, Wiley, New York, 1994, p. 498.
- [10] N.W. Ashcroft, N.D. Mermin, Solid-State Physics, Harcourt College Publishers, 2001, p. 656.
- [11] A. Abragam, B. Bleaney, Electron Paramagnetic Resonance of Transition Ions, Oxford, Clarendon, 1970.
- [12] I. Ardelean, Gh. Ilonca, M. Peteanu, E. Barbos, J. Mater. Sci. 17 (1982) 1988.
- [13] R.P. Sreekanth Chakradhar, J.L. Rao, G. Sivaramaiah, N.O. Gopal, Phys. Status Solidi (b) 242 (2005) 2929.
- [14] A. Srinivasa Rao, J. Lakshmana Rao, S.V.J. Lakshman, Solid State Commun. 85 (1993) 529.
- [15] C.R. Kesavulu, R.P.S. Chakradhar, R.S. Muralidhara, J.L. Rao, R.V. Anavekar, J. Alloys Compd. 496 (2010) 75.
- [16] I. Ardelean, O. Cozar, S. Filip, V. Pop, I. Ceanan, Solid State Commun. 100 (1996) 609.
- [17] J.T. Fournier, R.J. Landry, R.H. Bartram, J. Chem. Phys. 55 (1971) 2522.
- [18] A. Murali, J. Lakshmana Rao, J. Phys.: Condens. Matter 11 (1999) 1321.
- [19] G. Blasse, B. Grabmaier, Luminescent Materials, Springer, Berlin, 1995.
- [20] M. Casalbani, V. Ciafardone, G. Giuli, B. Izzi, E. Paris, P. Prosphito, J. Phys.: Condens. Matter. 8 (1996) 9059.
- [21] A.B.P. Lever, Inorganic Electronic Spectroscopy, 1968, p. 265.
- [22] M. Haouari, H. BenOuada, H. Maaref, H. Hommel, A.P. Legrand, J. Phys.: Condens. Matter 9 (1997) 6711.
- [23] J.W. Orton, An Introduction to Transition Group Ions in Crystals, ILLIFE Book Ltd, London, 1968.
- [24] R.P. Sreekanth Chakradhar, A. Murali, J. Lakshman Rao, J. Alloys Compd. 281 (1998) 99.
- [25] W. Seeber, D. Ehart, D. Eberdorff-Heidepriem, J. Non-Cryst. Solids 171 (1994) 94.
- [26] G. Little Flower, M. Srinivasa Reddy, G. Sahaya Baskaran, N. Veeriah, Opt. Mater. 30 (2007) 357.
- [27] W.A. Pisarski, J. Pisarska, G. Dominiak-Dzik, W. Ryba-Romanowski, J. Alloys Compd. 484 (2009) 45.
- [28] G. Fuxi, Optical and Spectroscopic Properties of Glass Berlin, Springer, 1992.
- [29] F. Rasheed, K.P. O'Donnell, B. Henderson, D.B. Hollis, J. Phys.: Condens. Matter 3 (1991) 1915.
- [30] F. Rasheed, K.P. O'Donnell, B. Henderson, D.B. Hollis, J. Phys.: Condens. Matter 3 (1991) 3825.
- [31] U.R. Rodriguez-Mendoza, V. Lavin, I.R. Martin, V.D. Rodriguez, J. Lumin. 106 (2004) 77.
- [32] C.R. Kesavulu, R.P.S. Chakradhar, C.K. Jayasankar, J.L. Rao, J. Mol. Struct. 975 (2010) 93.
- [33] W.M. Pontuschka, L.S. Kanashiro, L.C. Courrol, Glass Phys. Chem. 27 (2001) 37.